

1998

# Arginine to Glutamine Substitutions in the Fourth Module of *Xenopus* Interphotoreceptor Retinoid-Binding Protein

Mark S. Braiman

Syracuse University, mbraiman@syr.edu

Claxton A. Baer

Ellen E. Van Niel

Jeffrey W. Cronk

Michael T. Kinter

*See next page for additional authors*

Follow this and additional works at: <http://surface.syr.edu/che>

 Part of the [Chemistry Commons](#)

## Recommended Citation

Baer, C A & Van Niel, E E & Cronk, J W & Kinter, M T & Sherman, N E & Braiman, M S & Gonzalez-Fernandez, F. (1998). Arginine to glutamine substitutions in the fourth module of *Xenopus* interphotoreceptor retinoid-binding protein. *Molecular vision*, 4. Retrieved from <http://www.biomedsearch.com/nih/Arginine-to-glutamine-substitutions-in/9873068.html>

This Article is brought to you for free and open access by the College of Arts and Sciences at SURFACE. It has been accepted for inclusion in Chemistry Faculty Scholarship by an authorized administrator of SURFACE. For more information, please contact [surface@syr.edu](mailto:surface@syr.edu).

---

**Authors/Contributors**

Mark S. Braiman, Claxton A. Baer, Ellen E. Van Niel, Jeffrey W. Cronk, Michael T. Kinter, Nicholas E. Sherman, and Federico Gonzalez-Fernandez



# Arginine to Glutamine Substitutions in the Fourth Module of *Xenopus* Interphotoreceptor Retinoid-Binding Protein

Claxton A. Baer,<sup>1</sup> Ellen E. Van Niel,<sup>2</sup> Jeffrey W. Cronk,<sup>3</sup> Michael T. Kinter,<sup>4</sup> Nicholas E. Sherman,<sup>4</sup> Mark S. Braiman,<sup>1,5</sup> Federico Gonzalez-Fernandez<sup>1,2,3</sup>

<sup>1</sup>Graduate Program in Neuroscience, Departments of <sup>2</sup>Ophthalmology, <sup>3</sup>Pathology (Neuropathology), <sup>4</sup>Microbiology, and <sup>5</sup>Biochemistry, University of Virginia Health Sciences Center, Charlottesville, VA

**Purpose:** Interphotoreceptor retinoid-binding protein (*IRBP*) is unusual for a lipid-binding protein in that its gene is expressed uniquely by cells of photoreceptor origin and consists of four homologous repeats, each coding for a module of ~300 amino acid residues. All-*trans* retinol binding domains, which appear to be present in each module, are composed of conserved hydrophobic regions [Baer et al, *Exp Eye Res* 1998; 66:249-262]. Here we investigate the role of highly conserved arginines contained in these regions.

**Methods:** To study the arginines in an individual module without the interference of ligand-binding activity elsewhere in the protein, we expressed in *E. coli* the fourth module of *Xenopus* IRBP by itself as a soluble thioredoxin fusion protein (X4IRBP). Arginines 1005, 1041, 1073 and 1122 were separately replaced by glutamine using PCR overlap extension mutagenesis. The glutamine substitutions were confirmed by liquid chromatography-tandem mass spectrometry. The binding of all-*trans* retinol and 9-(9-anthroyloxy)stearic acid (9-AS) to X4IRBP and each of the mutants was evaluated by fluorescence spectroscopy. Binding was followed by monitoring the enhancement of ligand fluorescence and the quenching of protein endogenous fluorescence. The ability of the recombinant proteins to protect all-*trans* retinol from oxidative degradation was evaluated by monitoring absorbance at 325 nm over time.

**Results:** The substitution of Gln for Arg<sup>1005</sup> about doubled the amount of ligand necessary to attain saturation and about doubled the level of fluorescence enhancement obtained at saturation for both all-*trans* retinol and 9-AS. Although there was not a significant change in the  $K_d$ , the substitution increased the calculated number of binding sites (N) from ~2 to ~4 per polypeptide. The other Arg->Gln mutants did not significantly change the  $K_d$  or N. None of the mutations compromised the ability of the module to protect all-*trans* retinol from degradation.

**Conclusions:** Our data suggest that the function of the conserved arginines in IRBP is fundamentally different from that of other retinoid-binding proteins. These residues do not appear to play a role in defining the specificity of the ligand-binding domain. Rather, Arg<sup>1005</sup> appears to play a role in defining the capacity of the domain. Our data suggest that the binding site consists of a single hydrophobic cavity promiscuous for fatty acids and all-*trans*retinol.

Hydrophobic ligand-binding proteins transport diverse and potentially toxic molecules needed for critical biological processes (e. g. [1]). Interphotoreceptor retinoid-binding protein (IRBP) mediates the transport of 11-*cis* retinaldehyde and all-*trans* retinol between retinal pigment epithelium (RPE) and the photoreceptors (for reviews see [2-4]). IRBP provides a unique system to study how directional transport of different but structurally related ligands can be accomplished by the same protein.

IRBP is the most abundant soluble protein component of the extracellular material surrounding the photoreceptors and separating them from the RPE [5-11]. This material is known as the interphotoreceptor matrix. Unlike most retinoid-binding proteins present in a wide variety of tissues, IRBP expression is restricted to the retina and pineal gland [12-18]. It has

also been shown that IRBP is expressed by the RPE in zebrafish [19]. IRBP is large (124 kDa in *Xenopus*[20]) compared to other retinoid-binding proteins. Its large size is due to the fact that the IRBP gene is composed of multiple homologous repeats. Each repeat codes for a module of ~300 amino acid residues. Mammalian and amphibian *IRBPs* are composed of four repeats [21-24]. In contrast, teleost *IRBP* is composed of only two [25,26]. In all vertebrate classes examined to date, *IRBP*'s three introns are located in the repeat coding for the carboxy-terminal module (Figure 1A). This suggests that *IRBP* arose through the quadruplication of an ancestral gene composed of four exons [27,28].

Although it is not known how IRBP mediates the bi-directional transport of retinoids across the interphotoreceptor matrix, several important observations have been made. First, by binding retinoids, IRBP solubilizes and protects these molecules from isomeric and oxidative degradation [29]. Second, IRBP enhances the delivery of all-*trans*retinol from the rods to the RPE [30,31], and the transfer of 11-*cis*retinaldehyde from the RPE to the rods [31-35]. The mechanism by which IRBP promotes this bi-directional transport is not understood. A reduced affinity of 11-*cis* retinaldehyde for IRBP in the presence of docosahexaenoic acid may play a role in the delivery of this retinoid to the photoreceptors [36]. It also has been

Correspondence to: Federico Gonzalez-Fernandez, MD, PhD, Department of Ophthalmology, University of Virginia Health Sciences Center, P. O. Box 10009, Charlottesville, VA, 22906-0009; Phone: (804) 924-5717; Fax: (804) 924-9662; email: [fg2z@virginia.edu](mailto:fg2z@virginia.edu)  
Dr. Cronk is now at the Department of Internal Medicine, University of Virginia Health Sciences Center, Charlottesville, VA, 22908.  
Dr. Braiman is now at the Department of Chemistry, Room 1-014, Center for Science and Technology, Syracuse University, Syracuse, NY 13210.

postulated that IRBP functions by interacting with cell surface or matrix receptors [34,37].

Insights gained from phylogenetic alignments combined with recombinant protein expression technology are providing new information on the relationship between IRBP's structure and its function. An emerging picture is that the protein's biochemical [38-40] and physiological activity [41] is contained within each of the protein's individual modules. This suggests that there could be advantages in performing site directed mutagenesis studies in the isolated modules rather than in the full-length protein. In this way, the effect of specific substitutions on the ligand-binding properties of individual domains may be studied without the presence of binding sites in other modules. This could be especially helpful for binding studies employing fluorescence spectroscopy since nonequivalency of the binding sites and internal quenching can complicate the interpretation of such ligand-binding assays (see [42]).

We are using the African clawed frog (*Xenopus laevis*) because this animal has potential advantages for uncovering the relationship between the structure and function of IRBP. First, *Xenopus* IRBP has a 4-module structure similar to that of human IRBP [24]. *Xenopus* are easily cared for under different lighting conditions and their large inner segments facilitate morphological analysis. Furthermore, *Xenopus* eye-cups are metabolically active for extended periods. Unlike other amphibians and teleosts, the *Xenopus* retina can be detached in both light- and dark-adapted animals. Remarkably, the detached retina may be re-constituted allowing the introduction of molecules into the adult subretinal space [41,43]. Molecules may also be introduced into the subretinal space of the embryonic *Xenopus* retina through optic vesicle injections [44,45]. Finally, the *Xenopus* retina is particularly amenable to transgenic technology [46,47].

The fourth module of *Xenopus* IRBP as well as regions of the module corresponding to its exon segments are readily

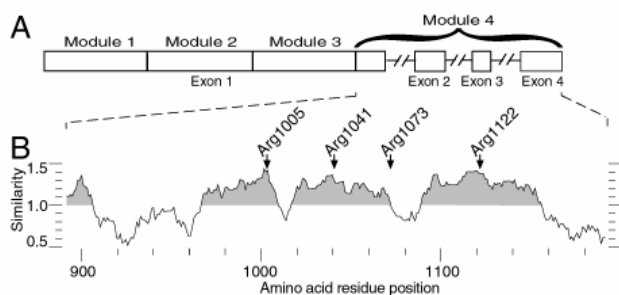


Figure 1. Summary of IRBP gene structure and location of the Arg->Gln substitutions. (A) Map of the IRBP gene with exons represented as rectangles and introns as interrupted lines. The first exon codes for protein modules 1 through 3 and part of module 4. The remainder of the fourth module is composed of segments derived from exons 2 through 4. Each module consists of ~300 amino acid residues. (B) Similarity plot of the C-terminal modules of human [22], bovine [27], *Xenopus* [20] and zebrafish [26] IRBPs. The stippled regions under the plot have a similarity score > 1.0. The positions of the Arg->Gln substitutions presented in this paper are indicated. Portions of this figure have been modified from Baer et al. [48].

expressed as soluble thioredoxin-fusion proteins [48]. We found that all-*trans*retinol binds to two regions within the fourth IRBP module. One of these sites is localized to Exons (2+3), and the other to Exon 4. Exon 1 has no retinol-binding activity. The potential importance of Exons 2 through 4 in the formation of the retinoid-binding site(s) is emphasized by their similarity with the newly recognized family of C-terminal processing proteases (CtpAs) [49]. CtpAs, which have only been described in plants and prokaryotes, selectively degrade proteins with nonpolar C-termini. It is possible that IRBP's hydrophobic ligand-binding sites are composed of domains derived from CtpAs.

CtpAs and IRBPs share three highly conserved hydrophobic regions [20,26,48,50]. IRBP Exons (2+3) contain two of the conserved hydrophobic segments, and Exon 4 contains one [48]. There is no significant similarity between the CtpAs and the Exon 1 region of module 4. In CtpAs, the conserved domains are responsible for recognition and cleavage of hydrophobic C-termini. Mutagenesis studies suggest that arginines within the conserved domains form salt bridges with aspartic acid residues critical to the recognition signal in the D1 precursor protein [51]. The fact that the arginine residues contained within the conserved IRBP domains are perfectly conserved between teleost, amphibian and mammalian IRBPs suggests that they may also be critical to the function of IRBP.

In lipocalins, mutagenesis and X-ray crystallographic studies have shown that arginine can confer specificity for retinoic and fatty acids by providing its guanidinium group to stabilize the carboxylate anion of these ligands [52-55]. Arginine has a similar role in the binding pocket of retinoic acid receptors [56,57]. The importance of arginines to retinoid-binding proteins is further emphasized by the recent finding that substitution of Gln for Arg<sup>150</sup> in cellular retinaldehyde-binding protein (CRALBP) causes autosomal recessive retinitis pigmentosa [58]. This substitution in CRALBP appears to interfere with its ability to bind 11-*cis* retinaldehyde, presumably leading to disruption of vitamin A metabolism in this disease.

The function of the conserved IRBP arginines is not known. Here, we selected the four most conserved arginines within the fourth *Xenopus* IRBP module for substitution studies. The position of each of these arginines (Arg<sup>1005</sup>, Arg<sup>1041</sup>, Arg<sup>1073</sup> and Arg<sup>1122</sup>) is identified in Figure 1B. We replaced Gln for Arg at each of these sites, expressed each of the mutants in *E. coli*, and compared their ligand-binding properties for 9-(9-anthroxloxy) stearic acid (9-AS) and all-*trans* retinol.

## METHODS

**PCR site-directed mutagenesis, expression and purification:** The fourth module of *Xenopus* IRBP (X4IRBP) and its mutants were expressed and purified as thioredoxin fusion proteins. The cDNA B1.B1 corresponding to the fourth module has been described [20] and used to express this module as polyhistidine [59] and thioredoxin fusion proteins [48]. This same cDNA was used to create arginine to glutamine substitutions at positions 1005, 1041, 1073 and 1122. These numbers correspond to the full-length *Xenopus* IRBP (Genbank accession number X95473). The mutations were introduced

by PCR overlap extension mutagenesis [60]. The oligonucleotide primers and mutagenesis strategy are summarized in Figure 2A,B. All plasmid constructs were transformed into GI724 *E. coli* [61].

Descriptions of overlap extension PCR do not mention a common pitfall. PCR can introduce an adenosine nucleotide at the 3' end of each strand produced. If allowed to remain, these "A overhangs" will be incorporated into the final PCR overlap extension product. The initial PCR product was therefore treated with T4 DNA polymerase to remove the A overhangs. Furthermore, the PCR primers were designed so that their 3' end is 5' to an adenosine. In this way, if an A overhang remained it would not cause a mutation. The sequence of each construct was confirmed by automated fluorescence DNA sequencing (Figure 2C).

Fermentations were carried out as previously described [48]. A 7-liter fermentor (Applikon, Foster City, CA) was used to grow the cells at 37 °C in induction media. After the cells reached an OD<sub>550</sub> of 0.5, the growth temperature was lowered to 30-35 °C before protein expression was commenced by the addition of tryptophan. The cells were harvested by centrifugation, resuspended in lysis buffer (50 mM Tris pH 7.4, 100 mM NaCl), and ruptured with a French pressure cell. Protein purification was carried out at 4 °C in the presence of 1 mM phenylmethylsulfonyl-fluoride, 1.4 μM pepstatin A, 0.3 μM aprotinin, and 2 μM leupeptin (Sigma, St. Louis, MO). The lysate was cleared by centrifugation and treated with DNase I (Sigma). The fusion proteins were precipitated from the supernatant with ammonium sulfate and further purified by ion exchange chromatography using a 200 mM to 850 mM NaCl linear gradient (Macro-Prep High Q Support, Bio-Rad, Hercules, CA). Purity, which ranged from 85-96%, was determined by laser densitometry (Molecular Dynamics, Sunnyvale, CA). The concentration of recombinant protein was determined by absorbance spectroscopy and amino acid analysis. Extinction coefficients were calculated from the translated amino acid sequence of the recombinant proteins [62]. To more accurately determine the concentration of IRBP in stocks used for ligand-binding assays, amino acid analysis was performed on a PICO-TAG system (Waters, Milford, MA) using phenylisothiocyanate derivatives [63]. Aliquots of the

purified thioredoxin fusion proteins in PBS (137 mM NaCl, 2.7 mM KCl, 4.3 mM Na<sub>2</sub>HPO<sub>4</sub>, 1.4 mM KH<sub>2</sub>PO<sub>4</sub>) were frozen in liquid N<sub>2</sub> and stored at -80 °C until use. We found no difference in the binding properties of X4IRBP that was frozen one time compared to that of freshly prepared material (data not illustrated). The frozen aliquots were never refrozen.

We have previously confirmed the sequence of X4IRBP by liquid chromatography-tandem mass spectrometry (LC-MS/MS) [48]. Here we used LC-MS/MS to confirm the Arg->Gln substitutions. Briefly, a Coomassie blue stained SDS-10% polyacrylamide gel slice containing approximately 3 μg of purified protein was treated with trypsin and the extracted proteolytic fragments analyzed by LC-MS to measure the mass to charge ratio of each fragment. The amino acid sequence of each of the detected fragments was then determined by collision activated dissociation mass spectrometry.

#### Fluorometric titrations and protection of all-trans retinol:

Enhancement of ligand fluorescence and quenching of the intrinsic protein fluorescence were used to monitor binding of 9-AS (Molecular Probes, Eugene, Oregon) and all-trans retinol (>99% purity; Acros Organics, Somerville, New Jersey) to the recombinant IRBPs. An extinction coefficient (ε) of 8,500 cm<sup>-1</sup>M<sup>-1</sup> at 361 nm in methanol was used to determine the 9-AS concentration [64]. For all-trans retinol we used the value of ε (38,300 cm<sup>-1</sup>M<sup>-1</sup> at 325 nm in ethanol) recently reported by Szuts and Harosi [65], who employed high performance liquid chromatography in their characterization of this retinoid. Titrations were performed by adding 0.5 μL aliquots of ligand in ethanol directly into the cuvette containing a 1 μM solution of recombinant protein. The solution was thoroughly mixed by inversion. Ligand aliquots were added at 1 min intervals unless otherwise stated. The final alcohol concentration never exceeded 2%. Measurements were made using an SLM 8000 C photon counting spectrofluorometer. Fluorescence enhancement was monitored at 440 nm exciting at 360 nm for 9-AS, and at 480 nm exciting at 330 nm for all-trans retinol. Quenching of endogenous protein fluorescence was monitored at 340 nm exciting at 280 nm. The protein quenching titrations were corrected for the inner filter effect as previously described [66]. The titration data were used to fit an equation described by Baer et al. [59]. For the enhancement titrations, the inner filter effect correction was not included because the ligand concentrations were sufficiently low. Purified recombinant *E. coli* thioredoxin was obtained from Promega (Madison, WI).

The ability of X4IRBP and the mutants to protect all-trans retinol from degradation was evaluated as described by Crouch et al. [29]. Briefly, the absorbance of all-trans retinol at 325 nm in the presence and absence of the recombinant protein was monitored as a function of time using a Hitachi U2000 spectrophotometer (Hitachi Instruments Inc., San Jose, CA).

## RESULTS

**Expression and purification:** Each of the Arg->Gln substitution mutants could be expressed in *E. coli* as a soluble thioredoxin fusion protein using conditions previously opti-

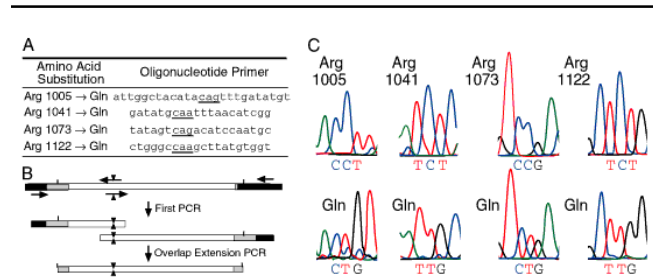


Figure 2. Creation of Arg->Gln substitution mutants by overlap extension mutagenesis. (A) The table provides the sense primers containing the mutated codon (underlined). (B) Diagram of the overlap PCR mutagenesis strategy (see Methods). (C) The mutants have been confirmed by automated fluorescence DNA sequencing. The sequences shown correspond to the non-coding strand.

mized for X4IRBP [48]. The yield after purification was ~15 mg (320 nmoles) per liter of culture. There was no apparent difference in the chromatographic behavior, yield, or solubility of the mutants compared to that of X4IRBP.

The replacement of Gln for Arg at positions 1005 and 1122 was directly confirmed by LC-MS/MS. Tryptic peptides containing amino acid residues 1005 and 1122, could be extracted from in-gel tryptic digests and identified by their mass to charge ratio (Figure 3). The amino acid sequence of these peptides was determined by collision-activated dissociation mass spectrometry. In contrast, tryptic peptides containing the Arg<sup>1041</sup>->Gln and Arg<sup>1073</sup>->Gln substitutions could not be identified. However these peptides, which have a large predicted size, either could not be extracted from the acrylamide, or could not be eluted from the reversed phase column. Since tryptic digests of the wild type protein generate peptides with C-terminal Arg<sup>1041</sup> and Arg<sup>1073</sup>, the absence of these peptides in the digests indicates that the desired substitutions were created.

**Binding of 9-AS:** The binding of 9-AS was monitored by following the enhancement of 9-AS fluorescence and quenching of protein endogenous fluorescence. In each experiment, titrations of X4IRBP were done along side that of the mutant. To confirm that the concentrations of X4IRBP and the mutants were the same, samples of the aliquots used in the fluorescence assays were run side by side on SDS-polyacrylamide gels. A representative set of gels is shown in Figure 4. Note that although each of the modules of IRBP are ~36 kDa in size, the fusion protein migrates with an  $M_r$  ~45 due to the presence of the thioredoxin fusion protein.

Compared to X4IRBP, the overall shape of the enhancement curves was not significantly changed by substituting Gln for Arg at positions 1041, 1073, and 1122 (Figure 5B-D). In contrast, although the initial slopes of the curves were similar for the Arg<sup>1005</sup>->Gln mutant and X4IRBP, this mutant required

about twice as much 9-AS to reach saturation (Figure 5A). Furthermore, this mutant attained twice the level of fluorescence enhancement at saturation compared to X4IRBP (see below). We have seen a similar effect for the same substitution expressed as a polyhistidine fusion protein within inclusion bodies (data not illustrated). Thus, the effect is not dependent on whether the protein is expressed in an insoluble form requiring renaturation, or in a soluble form as a thioredoxin fusion protein.

The dissociation constants ( $K_d$ ) of all four Arg->Gln mu-

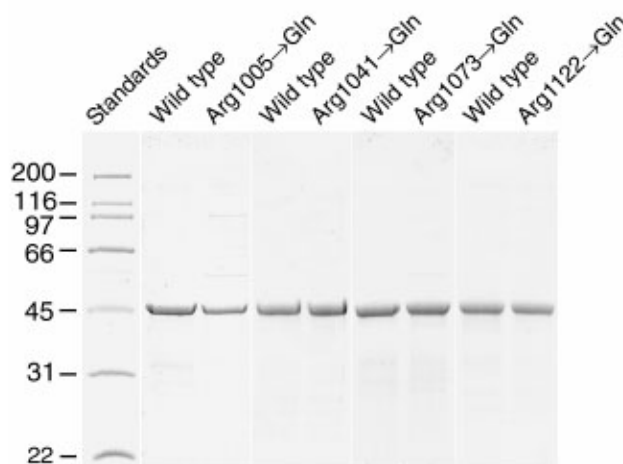


Figure 4. Coomassie blue stained SDS-10% polyacrylamide gels of purified recombinant X4IRBP and the four Arg->Gln mutants. In each panel X4IRBP was run along side one of the 4 Arg->Gln mutants (loading level = 5  $\mu$ g). All of the mutants were expressed in *E. coli* as soluble thioredoxin fusion proteins with similar yields as X4IRBP. The proteins shown here were purified by ammonium sulfate precipitation followed by ion exchange chromatography. The purity ranged from 85 to 96% based on densitometric scans of the Coomassie blue stained gels. The concentration of the protein was determined by amino acid analysis.

```

MSDKI IHLTDDSFDTDLVLLADGAILVDFWAHWCGPCMKIAPILDEIADEYQGKLTVAKLNIDHNPGTAPKYGIRGIPTLL
!
LFKNGEVAATKVGALSKGQLKEFLDANLAGSGSGDDDDKVPMELEIFEFRGRRGDPTKIPTVIQTAAKLVADNYAFADT
GANVASKFIALVDKIDYKMIKSEVELAEKINDDLQSLSKDFHLKAVYIPENSKDRIPGVVPMQIPSPELFEELIKFSFHT
*
DVFEKNIGYIQDFMADSDLLNQVSDLLVEHVWKKVVDQDALIDMRFNIGGPTSSIPFCSYFFDEGTPVLLDKIYSRT
-----
SNAMTDIWTLPDLVGKTFGSKKPLIILTSSLTEGAAEEFVYIMKRLGRAYVVGEVTSGGCHPPQTYHVDDTHLYLTIPTS
-----
RSASAEPGESWEGKGVLPDLEISSETALLKAKEILESQLEGRR

```

Figure 3. Confirmation of Arg<sup>1005</sup>->Gln substitution by liquid chromatography tandem mass spectrometry. This figure shows the amino acid sequence of the Arg<sup>1005</sup>->Gln thioredoxin fusion protein mutant. The exclamation mark (!) denotes the end of the thioredoxin fusion protein. The blue regions indicate the tryptic fragments that were identified by their mass to charge ratio. The amino acid sequences of these tryptic fragments were confirmed by collision-activated dissociation mass spectrometry. The asterisks (\*) denote the location of the four arginines that were mutated: (Arg<sup>1005</sup>, Arg<sup>1041</sup>, Arg<sup>1073</sup>, and Arg<sup>1122</sup>). The underlined regions are highly conserved between the carboxy-terminal modules of IRBPs and CtpAs [48].

tants were similar to that of X4IRBP which had a  $K_d$  of  $0.065 \pm 0.029 \mu\text{M}$  (Table 1). The number of binding sites in each mutant was also similar to that of X4IRBP except for Arg<sup>1005</sup>->Gln. This mutant had a significantly enhanced 9-AS binding capacity; X4IRBP and Arg<sup>1005</sup>->Gln bound  $1.88 \pm 0.06$  and  $4.27 \pm 0.09$  equivalents respectively.

The rate of 9-AS binding to X4IRBP and Arg<sup>1005</sup>->Gln is compared in Figure 6. The half time for 9-AS association to X4IRBP and Arg<sup>1005</sup>->Gln was 1.2 and 4.2 minutes respectively. To investigate whether the calculated binding capacity of the Arg<sup>1005</sup>->Gln mutant could have been overestimated due to the slower association rate, we allowed more time for equilibrium to be reached during the titrations. This was done by extending the time interval between the addition of each aliquot of 9-AS from 1 min to 25 min for Arg<sup>1005</sup>->Gln and to 7

min for X4IRBP. To obtain more data points near saturation, we extended the titration to  $\sim 9 \mu\text{M}$  9-AS compared to only  $\sim 4.5 \mu\text{M}$  in Figure 5. The titration is shown in Figure 7. Despite the additional time provided for equilibrium to be reached, the binding capacity of the Arg<sup>1005</sup>->Gln mutant remained high ( $N = 5.00 \pm 0.29$ ). For X4IRBP  $0.87 \pm 0.12$  binding sites were calculated compared to  $1.88 \pm 0.06$  in Figure 5. This reduction may be more apparent than real because fewer points are present in the dynamic range of the titration. The above results suggest that the enhanced binding capacity of the Arg<sup>1005</sup>->Gln mutant for 9-AS can not be attributed to an artifact related to its apparent lower association rate.

9-AS binding was also followed by monitoring protein fluorescence quenching (Figure 8). Despite the offsets, which are due to small differences in protein concentration, the overall

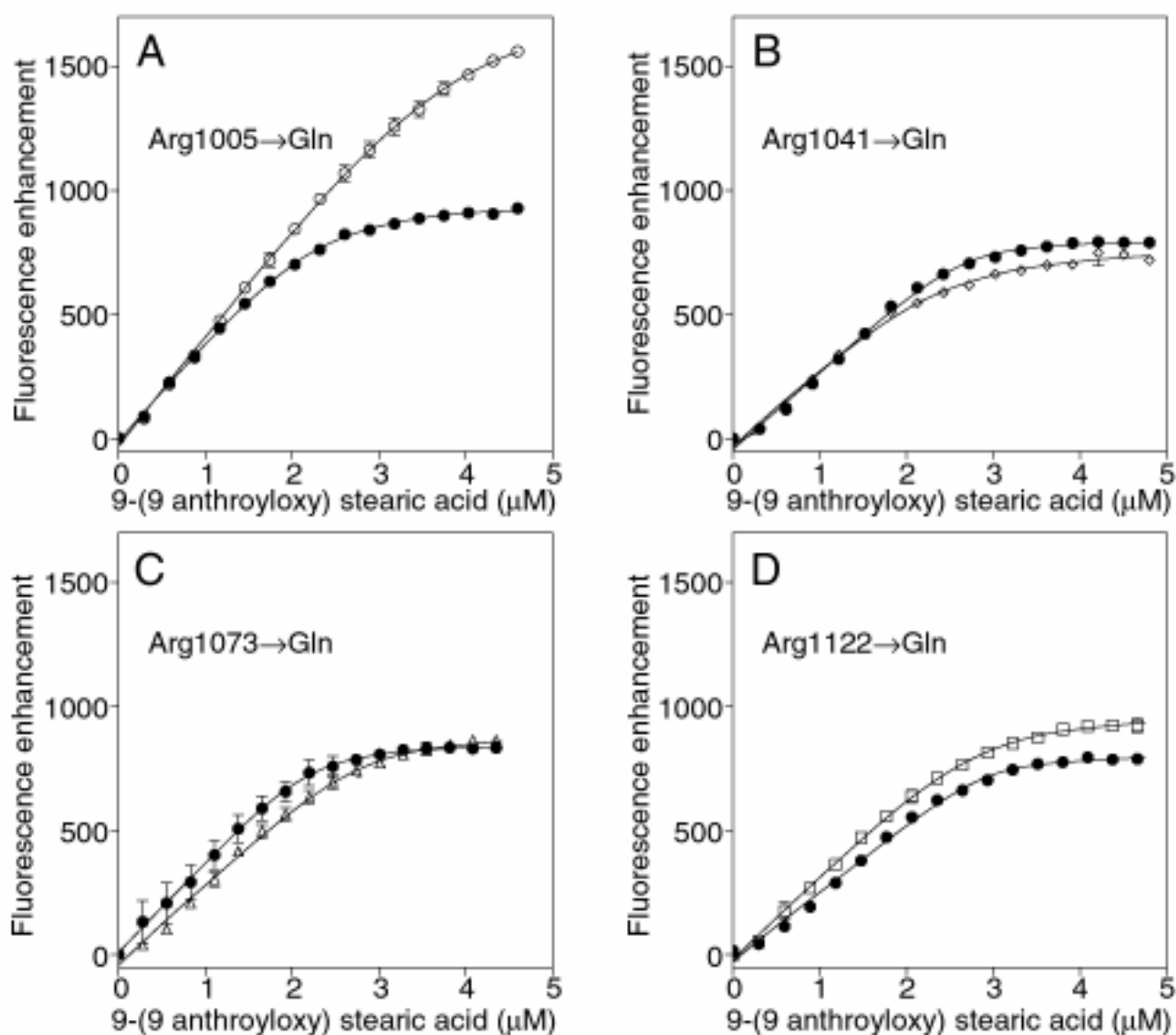


Figure 5. Binding of 9-AS to X4IRBP and the four Arg->Gln mutants monitoring fluorescence enhancement of 9-AS upon binding (excitation 360 nm; emission 440 nm). Each panel is a separate experiment comparing a single Arg->Gln mutant (open symbols) to that of module 4 of wild type sequence (filled symbols). The calculated binding parameters are summarized in Table 1. 9-AS binding to the Arg<sup>1005</sup>->Gln mutant required more 9-AS to reach saturation and had a markedly higher level of 9-AS fluorescence. Protein concentration was  $1 \mu\text{M}$ .

shape of the curves are similar for X4IRBP and each mutant. The  $K_d$ 's for X4IRBP and the four Arg->Gln substitution mutants were all in the submicromolar range (Table 2). Arg<sup>1005</sup>->Gln had an enhanced binding capacity compared to the other mutants and X4IRBP. The N's were lower for the titrations monitoring quenching compared to those monitoring enhancement. This effect is probably due to internal quenching (see Discussion).

**Binding and protection of all-trans retinol:** In Figure 9 the binding of all-trans retinol was followed by monitoring the enhancement of all-trans retinol fluorescence. As with 9-AS, the titrations of the four mutants were similar to each other and X4IRBP except for that of the Arg<sup>1005</sup>->Gln mutant. This Arg<sup>1005</sup>->Gln substitution approximately doubled the amount of all-trans retinol required to attain saturation ( $N = 1.28 \pm 0.19$ , X4IRBP;  $N = 2.95 \pm 0.19$  Arg<sup>1005</sup>->Gln). In contrast to N, the  $K_d$ 's were not significantly different for any of the proteins. Purified recombinant E. coli thioredoxin did not support all-trans retinol fluorescence enhancement, indicating that the fusion moiety does not alter binding.

A titration carried out to a higher all-trans retinol concentration is shown in Figure 10. Note, particularly for the normalized curves, that the Arg<sup>1005</sup>->Gln substitution required approximately twice as many moles of all-trans retinol as X4IRBP to attain saturation ( $N = 1.50 \pm 0.31$ , X4IRBP;  $N = 3.67 \pm 0.49$ , Arg<sup>1005</sup>->Gln). Although the number of binding sites for X4IRBP reported here is slightly less than  $2.20 \pm 0.39$  reported by Baer et al. [48], we still detected more than one binding site in X4IRBP. The  $K_d$  for all-trans retinol binding to X4IRBP was similar to that reported by Baer et al. [48]. The  $K_d$ 's of all four mutants were not significantly different from that of X4IRBP.

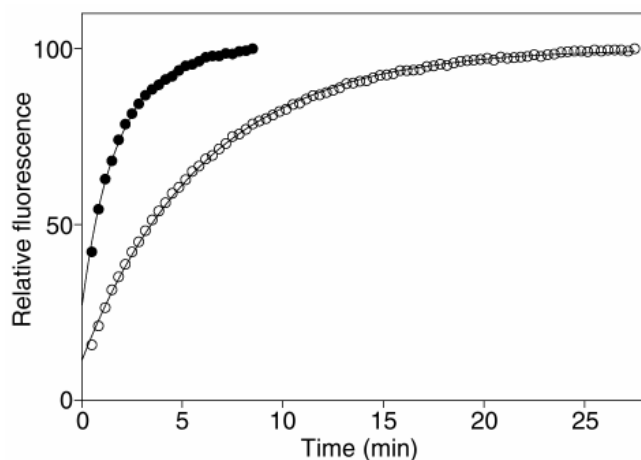


Figure 6. Normalized association curves of 9-AS with X4IRBP and the Arg<sup>1005</sup>->Gln mutant monitored by fluorescence over time. The association curve of X4IRBP (filled symbols) shows the increase in absolute fluorescence after addition of 0.92  $\mu$ M 9-AS to 1.3  $\mu$ M X4IRBP. The association curve of Arg<sup>1005</sup>->Gln (open symbols) shows the increase in absolute fluorescence after the addition of 0.96  $\mu$ M 9-AS to 0.92  $\mu$ M Arg<sup>1005</sup>->Gln. In both cases fluorescence was monitored at 440 nm upon excitation at 360 nm. The half-time for association increased from 1.24 min for X4IRBP to 4.19 min for the Arg<sup>1005</sup>->Gln mutant.

Emission spectra of X4IRBP and the Arg<sup>1005</sup>->Gln mutant in the presence and absence of all-trans retinol are shown in Figure 11. No significant difference was found in the emission spectra of these two proteins. Protein quenching is represented by the decrease in fluorescence emission at 340 nm. The emission at ~480 nm can be accounted for by the absorbance of all-trans retinol at 280 nm. Although the absorbance maximum for all-trans retinol is 325 nm, this ligand does absorb at 280 nm, the wavelength used to excite the protein. Consequently upon excitation at 280 nm, all-trans retinol will have some fluorescence at 480 nm as indicated by the small peak at 480 nm in Figure 11. The size of the 480 nm peak can be largely accounted for by this fluorescence (calculation not shown), and therefore does not represent transfer of energy from the protein to its bound ligand.

TABLE 1. SUMMARY OF BINDING PARAMETERS DETERMINED BY FLUORESCENCE ENHANCEMENT TITRATIONS

Protein	9-AS Enhancement*		All-trans retinol Enhancement#	
	N	Kd	N	Kd
X4IRBP	1.88±0.06	0.065±0.029 $\mu$ M	1.28±0.19	0.72±0.18 $\mu$ M
Arg1005->Gln	4.27±0.09	0.16 ±0.06 $\mu$ M	2.95±0.15	0.80±0.11 $\mu$ M
Arg1041->Gln	2.10±0.17	0.19 ±0.11 $\mu$ M	0.76±0.30	1.36±0.31 $\mu$ M
Arg1073->Gln	2.59±0.09	0.083±0.047 $\mu$ M	1.38±0.30	0.92±0.25 $\mu$ M
Arg1122->Gln	2.18±0.06	0.11 ±0.04 $\mu$ M	1.15±0.21	1.36±0.26 $\mu$ M

\* Monitored at 440 nm upon excitation at 360 nm.

# Monitored at 480 nm upon excitation at 330 nm.

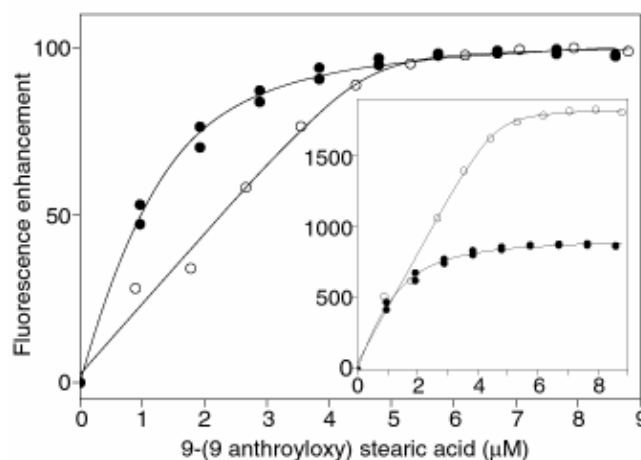


Figure 7. Normalized 9-AS fluorescence enhancement titrations comparing X4IRBP and the Arg<sup>1005</sup>->Gln mutant. The binding of 9-AS to 1.33  $\mu$ M of X4IRBP (filled symbols) and 0.92  $\mu$ M of the Arg<sup>1005</sup>->Gln mutant (open symbols) was monitored at 440 nm upon excitation at 360 nm. For X4IRBP,  $N = 0.87 \pm 0.12$  and  $K_d = 0.51 \pm 0.09$   $\mu$ M. For Arg<sup>1005</sup>->Gln,  $N = 5.00 \pm 0.29$  and  $K_d = 0.05 \pm 0.07$   $\mu$ M. Nonnormalized data is shown as an insert.

Protein fluorescence quenching was also used to monitor the binding of all-*trans* retinol. The overall shape of the titration curves and level of quenching achieved at saturation were similar for each protein except for the Arg<sup>1005</sup>->Gln mutant (Figure 12). This mutant had a slightly greater level of quenching compared to that of X4IRBP (Figure 12A). This is reflected in its higher number of binding equivalents ( $N = 0.51 \pm 0.11$ , Arg<sup>1005</sup>->Gln;  $N = 0.15 \pm 0.08$ , X4IRBP). The Arg<sup>1005</sup>->Gln mutant also had a slightly increased affinity for all-*trans* retinol compared to that of X4IRBP and the other three Arg->Gln mutants (Table 2). There were no significant differences in the  $K_d$ 's of the other three mutants compared to that of X4IRBP (Table 2). In panel B, the offset in the titration curves was due to a small difference in protein concentration between

X4IRBP and the mutant.  $N$  was less for titrations monitoring quenching compared to those monitoring enhancement probably due to internal quenching (see Discussion).

Protection of all-*trans* retinol from degradation in the presence of the recombinant IRBPs was evaluated by monitoring the absorbance of retinol at 325 nm as a function of time. The ability of X4IRBP and the mutants to protect all-*trans* retinol is compared in Figure 13. For a control the stability of all-*trans* retinol in PBS was assessed. Only ~60% of the original absorbance of all-*trans* retinol at 325 nm remained after 2 h in the absence of an IRBP. Compared to the PBS control, all four of the Arg->Gln substitution mutants and X4IRBP greatly reduced the rate of decline of absorbance at 325 nm.

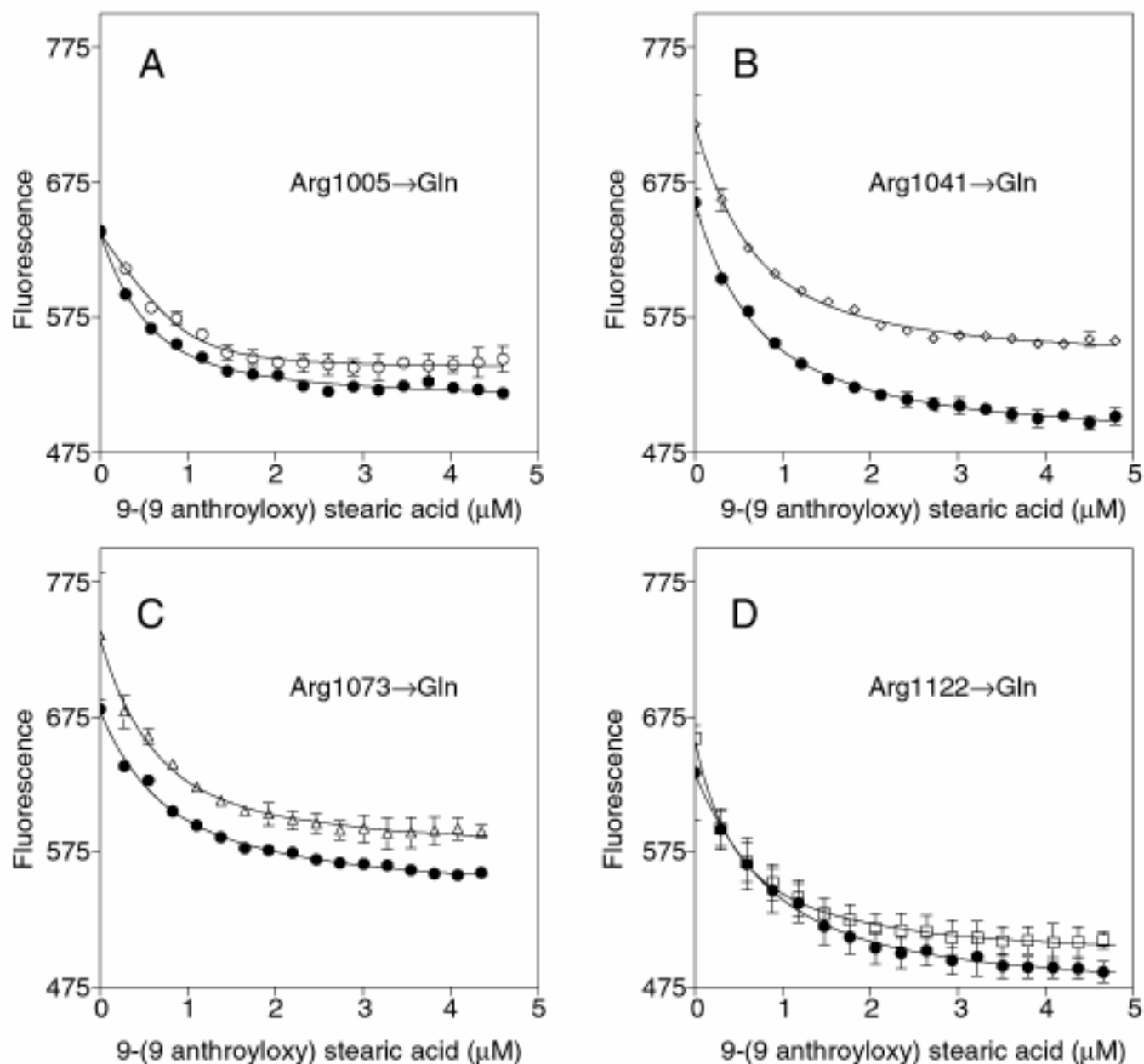


Figure 8. Binding of 9-AS to X4IRBP and the four Arg->Gln mutants monitoring quenching of protein fluorescence (excitation 280 nm; emission 340 nm). Each panel is a separate experiment comparing a single Arg->Gln substitution (open symbols) to that of X4IRBP (filled symbols). Note that the shape of the quenching curves is similar for X4IRBP and the mutants. Protein concentration was 1  $\mu$ M.

## DISCUSSION

We have expressed X4IRBP and the Arg<sup>1005</sup>->Gln substitution mutant in two *E. coli*-based systems. When expressed with polyhistidine tags in the pRSET system, both proteins were insoluble, requiring renaturation from inclusion bodies. The remarkable feature of the thioredoxin fusion protein system was that the proteins were expressed primarily in a soluble form. Thioredoxin enhances the solubility of a variety of proteins in *E. coli*. It does this by facilitating the reduction of abnormal disulfide bonds in partly folded intermediates [67,68]. The relative amount of protein in the soluble fraction can be further increased by optimizing the temperature of protein induction [48,61]. For X4IRBP and the substitution mu-

tants described here, lowering the incubation temperature from 37 °C to 30-32 °C before inducing expression significantly enhanced the yield of soluble protein. This phenomenon, which is not unique to thioredoxin fusion proteins, may be due to lower temperatures slowing the rate of protein production thus providing more time for limiting amounts of chaperone proteins to refold the overexpressed recombinant protein.

Mutagenesis studies typically rely only on DNA sequencing to confirm the desired mutation. LC-MS/MS allows for a higher level of confidence. We previously used LC-MS/MS to sequence peptides generated from in-gel trypsin digests of X4IRBP [48]. Each of these peptides could be matched to IRBP or thioredoxin with a 60% coverage of the fusion protein. In the present study, we found that the same peptides can

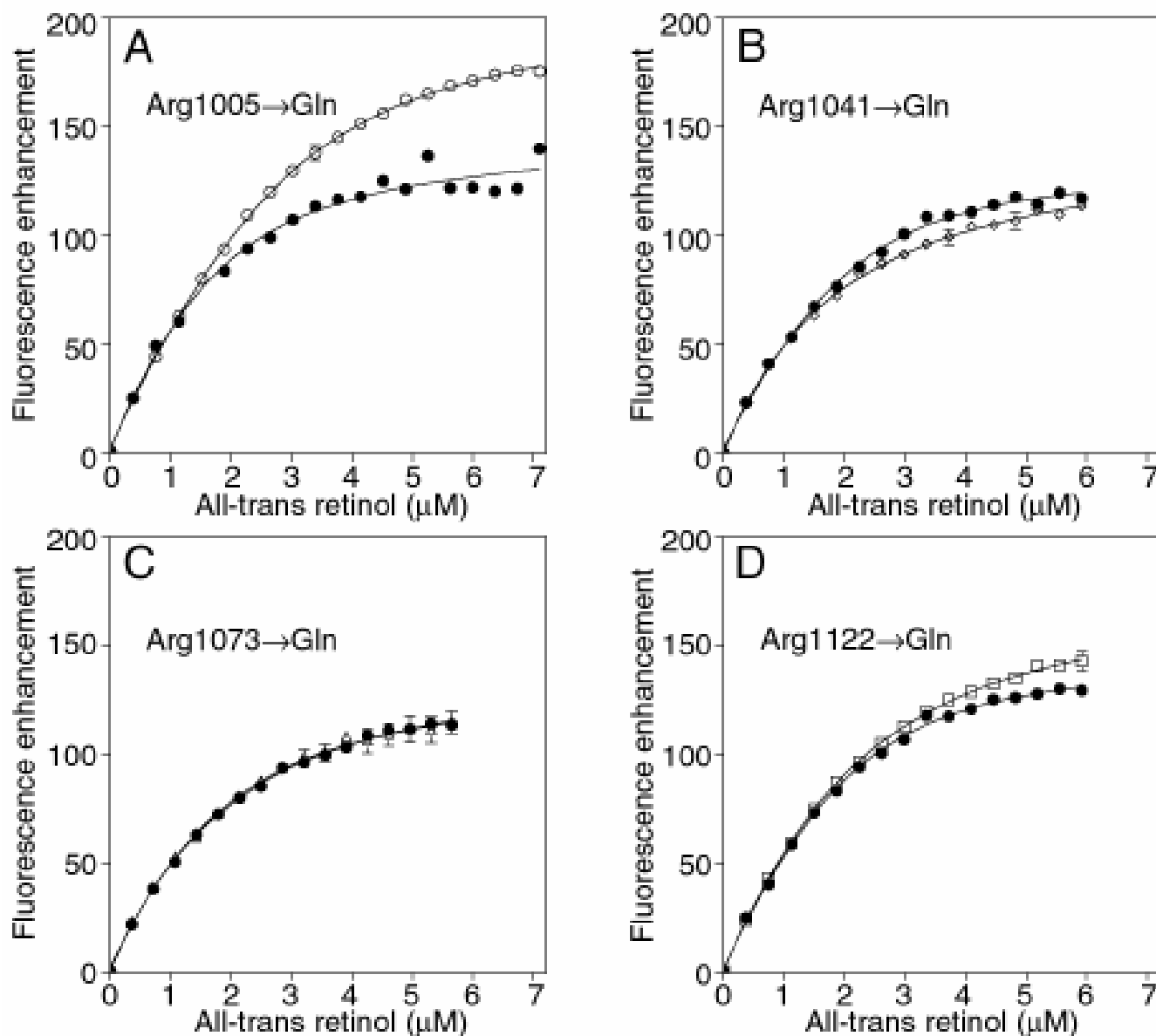


Figure 9. Binding of all-trans retinol to X4IRBP and the Arg->Gln mutants followed by monitoring ligand fluorescence enhancement upon binding (excitation 325 nm; emission 480 nm). Each panel is a separate experiment comparing a single Arg->Gln mutant (open symbols) to that of X4IRBP (filled symbols). The binding curves are similar except for the Arg<sup>1005</sup>->Gln mutant where more ligand was required to reach saturation and the level of fluorescence enhancement attained was higher (panel A). Protein concentration was 1 μM.

generally be isolated from the digest if the mutation has not disrupted the trypsin cleavage sites. Since trypsin cuts at arginine, the peptide profile was different for each of the mutants compared to X4IRBP. For Arg<sup>1005</sup>->Gln and Arg<sup>1122</sup>->Gln, a new peptide could be isolated that contained the desired amino acid substitution. For Arg<sup>1041</sup>->Gln and Arg<sup>1073</sup>->Gln the increased size of the resulting tryptic peptide precluded its direct characterization by LC-MS/MS.

Since the individual modules may represent functional units of IRBP each containing its own ligand-binding site(s) [38-40,48], studying the effect of mutations in isolated modules may be more useful than in the whole protein. Subtle effects of the mutation may be more easily identified without the presence of binding sites in other modules. Limitations of fluorescence spectroscopy may be circumvented by examining the modules individually. Since each module has different properties [38-40], the assumption of equivalent binding sites is not valid when studying the full-length IRBP. Furthermore, as pointed out by Ward [42]:

If the effect of ligand binding does affect the fluorescent properties of other binding sites, a nonlinear dependence of fluorescent change on fractional occupancy would result even for equivalent and independent binding sites. This type of effect could be caused by a conformational change on ligand binding affecting the fluorescent properties associated with consequent binding of ligand or via fluorescent energy transfer.

Such a mechanism accounts for the nonlinear quenching of the intrinsic protein fluorescence of lactate dehydrogenase on binding of NADH [69] and BSA on binding of 1-anilino-

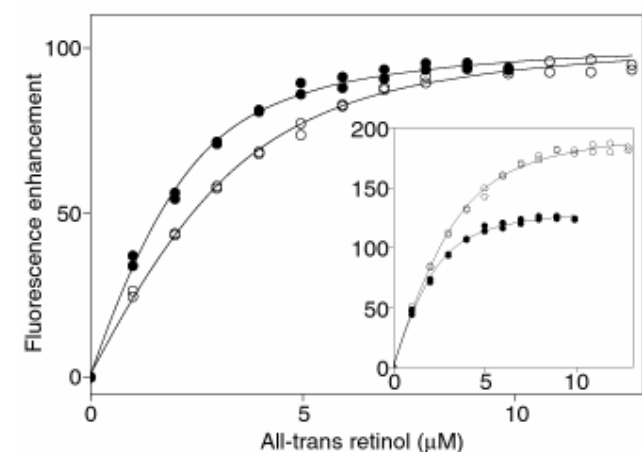


Figure 10. Normalized all-trans retinol fluorescence enhancement titrations showing direct comparison between X4IRBP and the Arg<sup>1005</sup>->Gln mutant. The binding of all-trans retinol to 1.33 μM of X4IRBP (filled symbols) and 0.92 μM of the Arg<sup>1005</sup>->Gln mutant (open symbols) was monitored at 480 nm upon excitation at 330 nm. For X4IRBP, N = 1.50±0.31 and K<sub>d</sub> = 0.80±0.26 μM. For Arg<sup>1005</sup>->Gln, N = 3.67±0.49 and K<sub>d</sub> = 0.93±0.26 μM. Nonnormalized data is shown as an insert.

8-naphthalene sulfonate (reviewed in [42]). In the present study, such internal quenching could explain why N determined from titrations following quenching of intrinsic protein fluorescence was less than N determined from titrations monitoring ligand fluorescence enhancement. An alternative explanation is that not all the binding sites support protein quenching.

In a screen of patients with retinitis pigmentosa, McGee et al. [70] found several point mutations in human IRBP that did not segregate with disease. None of these mutations correspond to the substitutions made in the present study. Lin et al. [38] studied two amino acid substitutions in human IRBP: Arg<sup>725</sup>->Cys and Gly<sup>719</sup>->Ser. Although Arg<sup>725</sup>->Cys does not correspond directly to any of the mutations made here, this amino acid residue in the third module of human IRBP corresponds to Arg<sup>1005</sup> in the fourth module of *Xenopus* IRBP. Al-

TABLE 2. SUMMARY OF BINDING PARAMETERS DETERMINED BY QUENCHING TITRATIONS

The binding of 9-(9-anthroyloxy) stearic acid (9-AS) and all-trans retinol to X4IRBP and the Arg->Gln substitution mutants was followed by monitoring quenching of protein endogenous fluorescence. The number of ligand-binding sites (N) and the dissociation constant (K<sub>d</sub>) were determined as described by Baer et al. [48].

Protein	9-AS Quenching*		All-trans retinol Quenching*	
	N	K <sub>d</sub>	N	K <sub>d</sub>
X4IRBP	0.24±0.10	0.46±0.08 μM	0.15±0.08	0.58±0.08 μM
Arg1005->Gln	1.06±0.18	0.10±0.06 μM	0.51±0.11	0.28±0.04 μM
Arg1041->Gln	0.32±0.13	0.38±0.09 μM	0.33±0.06	0.55±0.06 μM
Arg1073->Gln	0.39±0.16	0.36±0.09 μM	0.17±0.07	0.60±0.06 μM
Arg1122->Gln	0.12±0.07	0.35±0.05 μM	0.12±0.08	0.53±0.06 μM

\* Monitored at 340 nm upon excitation at 280 nm.

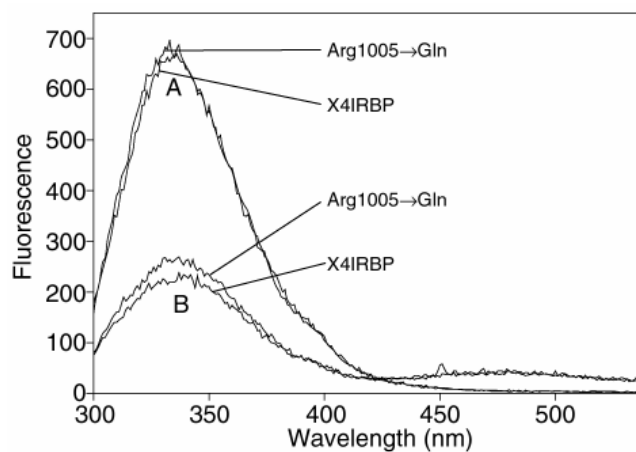


Figure 11. Emission spectra of X4IRBP and the Arg<sup>1005</sup>->Gln mutant showing the quenching of intrinsic protein fluorescence upon binding all-trans retinol. Solutions of 1 μM mutant and X4IRBP were excited at 280 nm. Emission was measured from 300 nm to 540 nm in the absence of all-trans retinol (A) and then five min after adding 7.1 μM all-trans retinol (B). Note the quenching of protein fluorescence at 340 nm upon addition of all-trans retinol.

though we saw a significant effect on ligand binding caused by changing this residue to glutamine, Lin et al. [38] found little effect on ligand binding by substituting Cys for Arg at residue 725. Although species differences may account for this apparent discrepancy, it is also possible that the difference reflects the different residue that the Arg was changed to and/or the fact that Lin et al. [38] examined the full-length protein while we studied an individual module.

Our results suggest that none of the Arg→Gln substitutions resulted in a global disruption of the module's structure. First, we found no reduction in the ability of any of the mutants to protect retinol from degradation, a property of IRBP that is regarded to be important in its function. Second, the substitutions did not appreciably change the  $K_d$  for 9-AS or all-*trans* retinol binding. It should be pointed out that for the most accurate determination of  $K_d$ , titrations should be carried out at a protein concentration that is less than the  $K_d$  (for discussion see [71]). Since the recombinant IRBPs were used

at 1  $\mu\text{M}$ , which is usually higher than the  $K_d$ s, we may have missed subtle changes caused by the substitutions. A more detailed analysis of the binding kinetics using stop-flow methodologies is underway in our laboratory.

In contrast to the lack of effect on  $K_d$ , substitution of Gln for Arg<sup>1005</sup> increased the amount of all-*trans* retinol or 9-AS required to reach saturation. Furthermore, the substitution approximately doubled the amount of fluorescence enhancement at saturation. The simplest explanation for these findings is that this substitution increased the module's ligand-binding capacity. The protein concentration used in these titrations was in an ideal range for evaluating the stoichiometry change. Fitting the ligand-binding equation, without any assumptions regarding how  $N$  or  $K_d$  should change, resulted in an approximate doubling of  $N$ . This doubling is supported by the fact that the level of fluorescence enhancement also doubled. Although a change in fluorescence enhancement could be caused by altering the hydrophobicity of the ligand-binding domain,

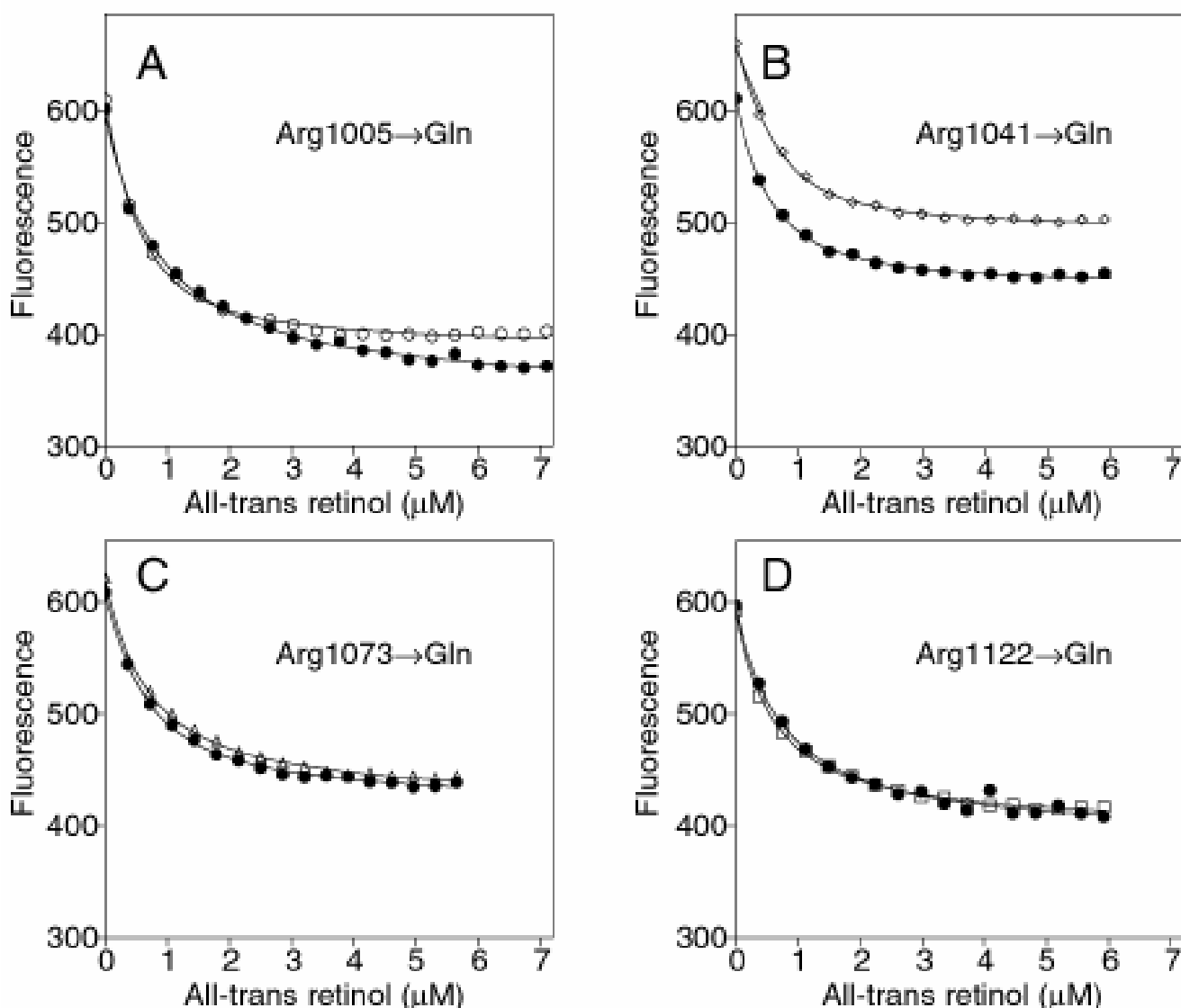


Figure 12. Binding of all-*trans* retinol to X4IRBP and the Arg→Gln mutants monitoring quenching of protein fluorescence (excitation 280 nm; emission 340 nm). Each panel is a separate experiment comparing a single Arg→Gln mutant (open symbol) to that of X4IRBP (filled symbol).

the large change observed is difficult to explain by a local environmental change alone. The apparent reduced rate of 9-AS association was considered as an explanation for the high value of  $N$ . However, the same result was obtained when even more time was allowed for equilibrium to be reached. Underestimating the protein concentration would also result in overestimating  $N$ . Absorbance spectroscopy can lead to errors in determining protein concentration due to inaccuracies in the extinction coefficient and the fact that contaminants can absorb at 280 nm. For these reasons we also employed amino acid analysis to determine the concentration of the IRBP used in the ligand-binding assays. The values obtained by the two methods were similar. SDS-PAGE analysis confirmed that the protein concentrations used in the side by side titrations of wild type and mutant were very similar (Figure 4).

In many lipocalins, conserved arginines form electrostatic interactions with bound ligand. For example, in cellular retinoic acid-binding protein, myelin P2, muscle fatty acid-binding protein, and intestinal fatty acid-binding protein, the carboxylate of the bound retinoic acid or fatty acid coordinates with specific conserved Arg residues [52-55]. In contrast, we found that the  $K_d$ 's for 9-AS and all-*trans* retinol binding were not significantly different for X4IRBP compared to that of any of the Arg->Gln mutants. The lack of notable ionic involvement of the conserved arginines studied here suggests that the mode of ligand binding in IRBP is different from that of the above lipocalins. This is consistent with the recent finding that the binding of retinol to native bovine IRBP is stabilized mainly by hydrophobic interactions [72].

Although our finding that substituting a Gln for an Arg can enhance binding capacity is unprecedented for a retinoid-binding protein or any lipocalin, a parallel may be drawn with liver fatty acid binding protein (L-FABP). Compared to other FABP's, which bind one molecule of long chain fatty acid, L-FABP binds two. The crystal structure of L-FABP suggests that the increase in binding capacity is due to a decrease in the

bulkiness of the amino acid side chains lining the binding cavity, thus increasing the volume of this cavity [73]. Mutagenesis of Arg<sup>122</sup> to Gln of L-FABP enhances its binding to lysophospholipids [74]. It is plausible that the enhanced binding of L-FABP (Arg<sup>122</sup>->Gln) and of Arg<sup>1005</sup>->Gln IRBP mutant produced here is the result of an increased flexibility of the binding cavity due to reduced hydrogen-bonding constraints resulting from the absence of the arginine.

## ACKNOWLEDGEMENTS

The authors thank Dr. Vladimir Kalashnikov and Dr. Yongbe Bao of the University of Virginia Biomedical Research Facility for determining the concentration of the purified recombinant IRBP by amino acid analysis and confirming the sequence of the expression plasmids by DNA sequencing. The Biomedical Research Facility is funded by the University of Virginia Pratt Committee. The University of Virginia Biomedical Mass Spectrometry Laboratory is funded in part by the W.M. Keck Foundation. Our study was supported by National Institutes of Health grants EY09412 (FG-F); The Thomas F. Jeffress and Kate Miller Memorial Trust (FG-F); Medical Scientist Training Program of the NIH GM 07267 (CAB); National Science Foundation instrumentation and instrument development grants BIR-901677 and BIR-9216996 to the Department of Biochemistry; and an unrestricted grant from Research to Prevent Blindness to the Department of Ophthalmology at the University of Virginia Health Sciences Center.

## REFERENCES

1. Flower DR. The lipocalin protein family: a role in cell regulation. *FEBS Lett* 1994; 354:7-11.
2. Pepperberg DR, Okajima TL, Wiggert B, Ripps H, Crouch RK, Chader GJ. Interphotoreceptor retinoid-binding protein (IRBP). Molecular biology and physiological role in the visual cycle of rhodopsin. *Mol Neurobiol* 1993; 7:61-85.
3. Saari JC. Retinoids in photosensitive systems. In: Sporn MB, Roberts AB, Goodman DS, editors. *The retinoids: biology, chemistry, and medicine*. New York: Raven Press; 1994. p. 351-85.
4. Crouch RK, Chader GJ, Wiggert B, Pepperberg DR. Retinoids and the visual process. *Photochem Photobiol* 1996; 64:613-21.
5. Adler AJ, Martin KJ. Retinol-binding proteins in bovine interphotoreceptor matrix. *Biochem Biophys Res Commun* 1982; 108:1601-8.
6. Adler AJ, Evans CD, Stafford WF 3d. Molecular properties of bovine interphotoreceptor retinol-binding protein. *J Biol Chem* 1985; 260:4850-5.
7. Fong SL, Liou GI, Landers RA, Alvarez RA, Gonzalez-Fernandez F, Glazebrook PA, Lam DM, Bridges CD. Characterization, localization, and biosynthesis of an interstitial retinol-binding glycoprotein in the human eye. *J Neurochem* 1984; 42:1667-76.
8. Lai YL, Wiggert B, Liu YP, Chader GJ. Interphotoreceptor retinoid-binding proteins: possible transport vehicles between compartments of the retina. *Nature* 1982; 298:848-9.
9. Liou GI, Bridges CD, Fong SL, Alvarez RA, Gonzalez-Fernandez F. Vitamin A transport between retina and pigment epithelium—an interstitial protein carrying endogenous retinol (interstitial retinol-binding protein). *Vision Res* 1982; 22:1457-67.
10. Pfeffer B, Wiggert B, Lee L, Zonnenberg B, Newsome D, Chader G. The presence of a soluble interphotoreceptor retinoid-binding protein (IRBP) in the retinal interphotoreceptor space. *J Cell Physiol* 1983; 117:333-41.

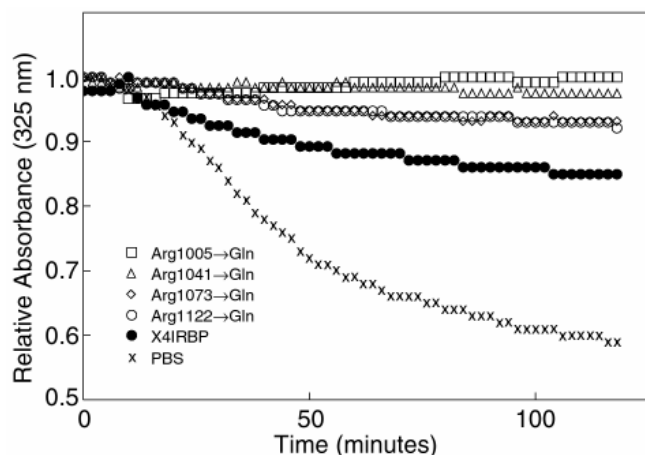


Figure 13. Protection of all-*trans* retinol by X4IRBP and the four Arg->Gln mutants. All-*trans* retinol was added to a solution of 2.7  $\mu$ M recombinant protein to a final concentration of 3.2  $\mu$ M. The absorbance of all-*trans* retinol was monitored at 325 nm every two min for 2 h. The ethanol concentration was 0.74%.

11. Saari JC, Teller DC, Crabb JW, Bredberg L. Properties of an interphotoreceptor retinoid-binding protein from bovine retina. *J Biol Chem* 1985; 260:195-201.
12. Hollyfield JG, Fliesler SJ, Rayborn ME, Bridges CD. Rod photoreceptors in the human retina synthesize and secrete interstitial retinol-binding protein. *Prog Clin Biol Res* 1985; 190:141-9.
13. van Veen T, Katial A, Shinohara T, Barrett DJ, Wiggert B, Chader GJ, Nickerson JM. Retinal photoreceptor neurons and pinealocytes accumulate mRNA for interphotoreceptor retinoid-binding protein (IRBP). *FEBS Lett* 1986; 208:133-7.
14. Gonzalez-Fernandez F, Lopes MB, Garcia-Fernandez JM, Foster RG, De Grip WJ, Rosemberg S, Newman SA, VandenBerg SR. Expression of developmentally defined retinal phenotypes in the histogenesis of retinoblastoma. *Am J Pathol* 1992; 141:363-75.
15. Yokoyama T, Liou GI, Caldwell RB, Overbeek PA. Photoreceptor-specific activity of the human interphotoreceptor retinoid-binding protein (IRBP) promoter in transgenic mice. *Exp Eye Res* 1992; 55:225-33.
16. Hessler RB, Baer CA, Bukelman A, Kittredge KL, Gonzalez-Fernandez F. Interphotoreceptor retinoid-binding protein (IRBP): expression in the adult and developing *Xenopus* retina. *J Comp Neurol* 1996; 367:329-41.
17. Porrello K, Bhat SP, Bok D. Detection of interphotoreceptor retinoid binding protein (IRBP) mRNA in human and cone-dominant squirrel retinas by in situ hybridization. *J Histochem Cytochem* 1991; 39:171-6.
18. Stenkamp DL, Barthel LK, Raymond PA. Spatiotemporal coordination of rod and cone photoreceptor differentiation in goldfish retina. *J Comp Neurol* 1997; 382:272-84.
19. Stenkamp DL, Cunningham LL, Raymond PA, Gonzalez-Fernandez F. Novel expression pattern of Interphotoreceptor retinoid-binding protein (IRBP) in the adult and developing zebrafish retina and RPE. *Mol Vis* 1998; 4:26 .
20. Gonzalez-Fernandez F, Kittredge KL, Rayborn ME, Hollyfield JG, Landers RA, Saha M, Grainger RM. Interphotoreceptor retinoid-binding protein (IRBP), a major 124 kDa glycoprotein in the interphotoreceptor matrix of *Xenopus laevis*. Characterization, molecular cloning and biosynthesis. *J Cell Sci* 1993; 105:7-21.
21. Liou GI, Ma DP, Yang YW, Geng L, Zhu C, Baehr W. Human interstitial retinoid-binding protein. Gene structure and primary structure. *J Biol Chem* 1989; 264:8200-6.
22. Si JS, Borst DE, Redmond TM, Nickerson JM. Cloning of cDNAs encoding human interphotoreceptor retinoid-binding protein (IRBP) and comparison with bovine IRBP sequences. *Gene* 1989; 80:99-108.
23. Fong SL, Fong WB, Morris TA, Kedzie KM, Bridges CD. Characterization and comparative structural features of the gene for human interstitial retinol-binding protein. *J Biol Chem* 1990; 265:3648-53.
24. Van Niel E, Wagenhorst B, Cronk J, Gonzalez-Fernandez F. Searching for functional domains within IRBP through phylogenetic comparisons and site-directed mutagenesis. *Invest Ophthalmol Vis Sci* 1993; 34:1197.
25. Wagenhorst BB, Rajendran RR, Van Niel EE, Hessler RB, Bukelman A, Gonzalez-Fernandez F. Goldfish cones secrete a two-repeat interphotoreceptor retinoid-binding protein. *J Mol Evol* 1995; 41:646-56.
26. Rajendran RR, Van Niel EE, Stenkamp DL, Cunningham LL, Raymond PA, Gonzalez-Fernandez F. Zebrafish interphotoreceptor retinoid-binding protein: differential circadian expression among cone subtypes. *J Exp Biol* 1996; 199:2775-87.
27. Borst DE, Redmond TM, Elser JE, Gonda MA, Wiggert B, Chader GJ, Nickerson JM. Interphotoreceptor retinoid-binding protein. Gene characterization, protein repeat structure, and its evolution. *J Biol Chem* 1989; 264:1115-23.
28. Nickerson JM, Borst DE, Redmond TM, Si JS, Toffenetti J, Chader GJ. The molecular biology of IRBP: application to problems of uveitis, protein chemistry, and evolution. *Prog Clin Biol Res* 1991; 362:139-61.
29. Crouch RK, Hazard ES, Lind T, Wiggert B, Chader G, Corson DW. Interphotoreceptor retinoid-binding protein and alpha-tocopherol preserve the isomeric and oxidation state of retinol. *Photochem Photobiol* 1992; 56:251-5.
30. Okajima TL, Pepperberg DR, Ripps H, Wiggert B, Chader GJ. Interphotoreceptor retinoid-binding protein: role in delivery of retinol to the pigment epithelium. *Exp Eye Res* 1989; 49:629-44.
31. Flannery JG, O'Day W, Pfeffer BA, Horwitz J, Bok D. Uptake, processing and release of retinoids by cultured human retinal pigment epithelium. *Exp Eye Res* 1990; 51:717-28.
32. Jones GJ, Crouch RK, Wiggert B, Cornwall MC, Chader GJ. Retinoid requirements for recovery of sensitivity after visual-pigment bleaching in isolated photoreceptors. *Proc Natl Acad Sci U S A* 1989; 86:9606-10.
33. Okajima TL, Pepperberg DR, Ripps H, Wiggert B, Chader GJ. Interphotoreceptor retinoid-binding protein promotes rhodopsin regeneration in toad photoreceptors. *Proc Natl Acad Sci U S A* 1990; 87:6907-11.
34. Carlson A, Bok D. Promotion of the release of 11-cis-retinal from cultured retinal pigment epithelium by interphotoreceptor retinoid-binding protein. *Biochemistry* 1992; 31:9056-62.
35. Duffy M, Sun Y, Wiggert B, Duncan T, Chader GJ, Ripps H. Interphotoreceptor retinoid binding protein (IRBP) enhances rhodopsin regeneration in the experimentally detached retina. *Exp Eye Res* 1993; 57:771-82.
36. Chen Y, Houghton LA, Brenna JT, Noy N. Docosahexaenoic acid modulates the interactions of the interphotoreceptor retinoid-binding protein with 11-cis retinal. *J Biol Chem* 1996; 271:20507-15.
37. Duncan T, Palmer K, Chader GJ, Wiggert B. A putative retinal pigment epithelial cell surface receptor for interphotoreceptor retinoid-binding protein (IRBP). *Invest Ophthalmol Vis Sci* 1995; 36:S122.
38. Lin ZY, Li GR, Takizawa N, Si JS, Gross EA, Richardson K, Nickerson JM. Structure-function relationships in interphotoreceptor retinoid-binding protein (IRBP). *Mol Vis* 1997; 3:17 .
39. Shaw NS, Liou GI, Noy N. Localization of the retinoid binding sites of human interphotoreceptor retinoid binding protein expressed in *E. coli*. *Invest Ophthalmol Vis Sci* 1998; 39:S40.
40. Van Niel EE, Baer CA, Gonzalez-Fernandez F. Structure/function studies of IRBP modules expressed as thioredoxin fusion proteins in *E. coli*. *Invest Ophthalmol Vis Sci* 1997; 38:S4.
41. Gonzalez-Fernandez F, Baer C, Baker E, Okajima TL, Wiggert B, Brainman M, Pepperberg DR. Fourth module of *Xenopus* interphotoreceptor retinoid-binding protein: activity in retinoid transfer between the retinal pigment epithelium and rod photoreceptors. *Cur Eye Res.* 1998; 17:1150-1157. <[http://www.oup.co.uk/cureye/hdb/Volume\\_17/Issue\\_12/](http://www.oup.co.uk/cureye/hdb/Volume_17/Issue_12/)>.
42. Ward LD. Measurement of ligand binding to proteins by fluorescence spectroscopy. *Methods Enzymol* 1985; 117:400-14.
43. Defoe DM, Matsumoto B, Besharse JC. Reconstitution of the photoreceptor-pigment epithelium interface: L-glutamate stimulation of adhesive interactions and rod disc shedding after re-

- combination of dissociated *Xenopus laevis* eyecups. *Exp Eye Res* 1992; 54:903-11.
44. Hollyfield JG, Witkovsky P. Pigmented retinal epithelium involvement in photoreceptor development and function. *J Exp Zool* 1974; 189:357-78.
  45. Gonzalez-Fernandez F, Kittredge KL. Getting into the embryonic subretinal space. *Invest Ophthalmol Vis Sci* 1992; 33:816.
  46. Kroll KL, Amaya E. Transgenic *Xenopus* embryos from sperm nuclear transplantations reveal FGF signaling requirements during gastrulation. *Development* 1996; 122:3173-83.
  47. Knox BE, Schlueter C, Sanger BM, Green CB, Besharse JC. Transgene expression in *Xenopus* rods. *FEBS Lett* 1998; 423:117-21.
  48. Baer CA, Retief JD, Van Niel E, Braiman MS, Gonzalez-Fernandez F. Soluble expression in *E. coli* of a functional interphotoreceptor retinoid-binding protein module fused to thioredoxin: correlation of vitmain A binding regions with conserved domains of C-terminal processing proteases. *Exp Eye Res* 1998; 66:249-62.
  49. Oelmuller R, Herrmann RG, Pakrasi HB. Molecular studies of CtpA, the carboxyl-terminal processing protease for the D1 protein of the photosystem II reaction center in higher plants. *J Biol Chem* 1996; 271:21848-52.
  50. Liou GI, Geng L, Baehr W. Interphotoreceptor retinoid-binding protein: biochemistry and molecular biology. *Prog Clin Biol Res* 1991; 362:115-37.
  51. Taguchi F, Yamamoto Y, Inagaki N, Satoh K. Recognition signal for the C-terminal processing protease of D1 precursor protein in the photosystem II reaction center. An analysis using synthetic oligopeptides. *FEBS Lett* 1993; 326:227-31.
  52. Sacchetti JC, Gordon JI, Banaszak LJ. Crystal structure of rat intestinal fatty-acid-binding protein. Refinement and analysis of the *Escherichia coli*-derived protein with bound palmitate. *J Mol Biol* 1989; 208:327-39.
  53. Cheng L, Qian SJ, Rothschild C, d'Avignon A, Lefkowitz JB, Gordon JI, Li E. Alteration of the binding specificity of cellular retinol-binding protein II by site-directed mutagenesis. *J Biol Chem* 1991; 266:24404-12.
  54. Stump DG, Lloyd RS, Chytil F. Site-directed mutagenesis of rat cellular retinol-binding protein. Alteration in binding specificity resulting from mutation of glutamine 108 to arginine. *J Biol Chem* 1991; 266:4622-30.
  55. Zhang J, Liu ZP, Jones TA, Gierasch LM, Sambrook JF. Mutating the charged residues in the binding pocket of cellular retinoic acid-binding protein simultaneously reduces its binding affinity to retinoic acid and increases its thermostability. *Protein* 1992; 13:87-99.
  56. Lamour FP, Lardelli P, Apfel CM. Analysis of the ligand-binding domain of human retinoic acid receptor alpha by site-directed mutagenesis. *Mol Cell Biol* 1996; 16:5386-92.
  57. Renaud JP, Rochel N, Ruff M, Vivat V, Chambon P, Gronemeyer H, Moras D. Crystal structure of the RAR-gamma ligand-binding domain bound to all-trans retinoic acid. *Nature* 1995; 378:681-9.
  58. Maw MA, Kennedy B, Knight A, Bridges R, Roth KE, Mani EJ, Mukkadan JK, Nancarrow D, Crabb JW, Denton MJ. Mutation of the gene encoding cellular retinaldehyde-binding protein in autosomal recessive retinitis pigmentosa. *Nat Genet* 1997; 17:198-200.
  59. Baer CA, Kittredge KL, Klinger AL, Briercheck DM, Braiman MS, Gonzalez-Fernandez F. Expression and characterization of the fourth repeat of *Xenopus* interphotoreceptor retinoid-binding protein in *E. coli*. *Curr Eye Res* 1994; 13:391-400.
  60. Horton RM. PCR-mediated recombination and mutagenesis. SOEing together tailor-made genes. *Mol Biotechnol* 1995; 3:93-9.
  61. McCoy JM, LaVallie ER. Expression and purification of thioredoxin fusion proteins. In: Ausubel FM, Brent R, Kingston RE, Moore DD, Seidman JG, Smith JA, Struhl K, editors. *Current protocols in molecular biology*. Vol 2. New York: John Wiley & Sons; 1994. p. 16.8.1-16.8.14.
  62. Gill SC, von Hippel PH. Calculation of protein extinction coefficients from amino acid sequence data. *Anal Biochem* 1989; 182:319-26.
  63. Cohen SA, Strydom DJ. Amino acid analysis utilizing phenylisothiocyanate derivatives. *Anal Biochem* 1988; 174:1-16.
  64. Haugland RP. Other fluorescent and thin-labeled fatty acids. In: Spence MTZ, editor. *Handbook of fluorescent probes and research chemicals*. 6th ed. Eugene (OR): Molecular Probes; 1996. p. 297-300.
  65. Szuts EZ, Harosi FI. Solubility of retinoids in water. *Arch Biochem Biophys* 1991; 287:297-304.
  66. Mertens ML, Kagi JH. A graphical correction procedure for inner filter effect in fluorescence quenching titrations. *Anal Biochem* 1979; 96:448-55.
  67. Yasukawa T, Kanei-Ishii C, Maekawa T, Fujimoto J, Yamamoto T, Ishii S. Increase of solubility of foreign proteins in *Escherichia coli* by coproduction of the bacterial thioredoxin. *J Bio Chem* 1995; 270:25328-31.
  68. Li W, Churchich JE. Activation of partially folded mitochondrial malate dehydrogenase by thioredoxin. *Eur J Biochem* 1997; 246:127-32.
  69. Holbrook JJ, Yates DW, Reynolds SJ, Evans RW, Greenwood C, Gore MG. Protein fluorescence of nicotinamide nucleotide-dependent dehydrogenases. *Biochem J* 1972; 128:933-40.
  70. McGee TL, DeStefano JD, Berson EL, Dryja TP. A complete screen of the entire coding sequence of the IRBP gene for mutations in patients with hereditary retinal degenerations. *Invest Ophthalmol Vis Sci* 1993; 34:1460.
  71. Norris AW, Cheng L, Giguere V, Rosenberger M, Li E. Measurement of subnanomolar retinoic acid binding affinities for cellular retinoic acid binding proteins by fluorometric titration. *Biochim Biophys Acta* 1994; 1209:10-8.
  72. Tschanz CL, Noy N. Binding of retinol in both retinoid-binding sites of interphotoreceptor retinoid-binding protein (IRBP) is stabilized mainly by hydrophobic interactions. *J Biol Chem* 1997; 272:30201-7.
  73. Thompson J, Winter N, Terwey D, Bratt J, Banaszak L. The crystal structure of the liver fatty acid-binding protein. A complex with two bound oleates. *J Biol Chem* 1997; 272:7140-50.
  74. Thumser AE, Wilton DC. The binding of natural and fluorescent lysophospholipids to wild-type and mutant rat liver fatty acid-binding protein and albumin. *Biochem J* 1995; 307:305-11.